The Abdus Salam International Centre for Theoretical Physics

United Nations Educational, Scientific and Cultural Organization

International Atomic Energy Agency

H4.SMR/1775-22

"8th Workshop on Three-Dimensional Modelling of Seismic Waves Generation, Propagation and their Inversion"

25 September - 7 October 2006

# From Experimental Hydraulic Fracturing to the *in situ* characterization of rheological characteristics of rock masses

*F. H. Cornet*

**Institute de Physique du Globe de Paris**
**France**

Strada Costiera 11, 34014 Trieste, Italy - Tel. +39 040 2240 111; Fax +39 040 224 163 - sci_info@ictp.it, www.ictp.it

# From Experimental Hydraulic Fracturing to the *in situ* characterization of rheological characteristics of rock masses

# The European Experimental Hot Dry Rock site at Soultz

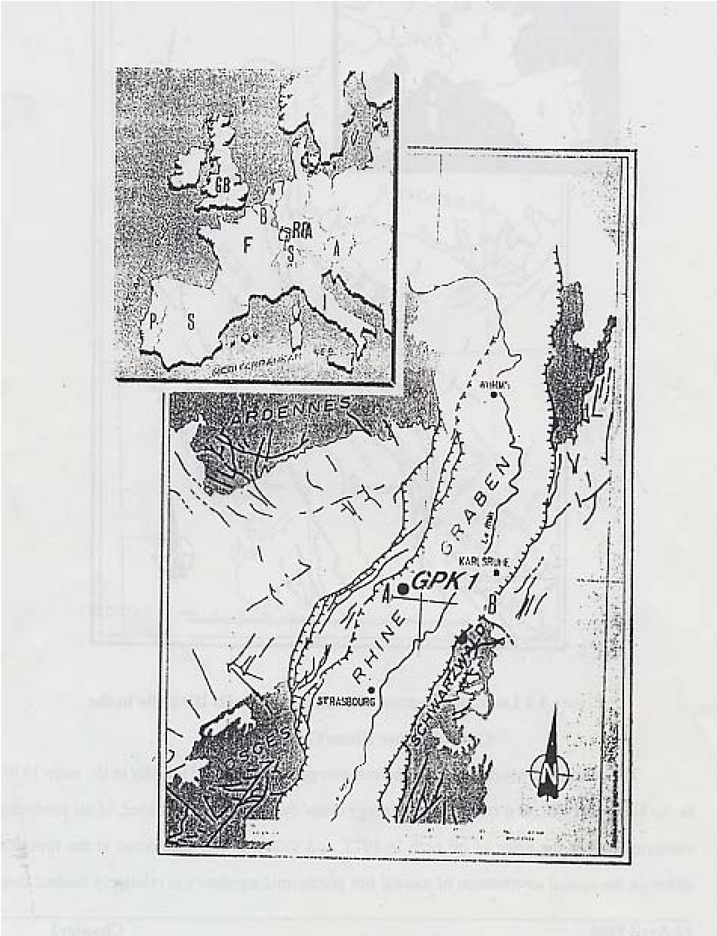


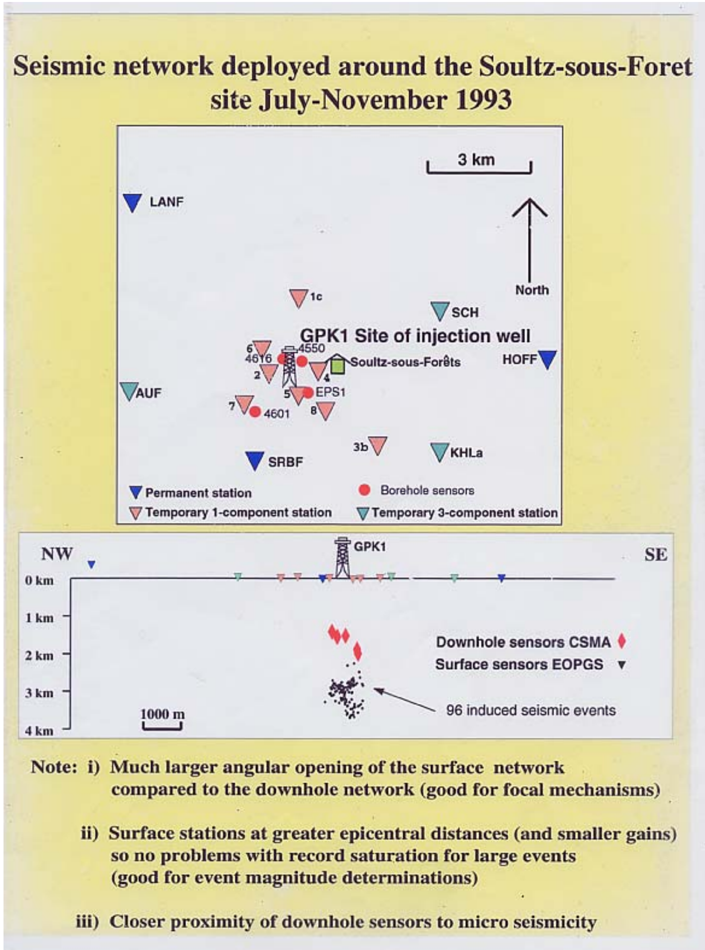

# Analysis of drilling induced fracture

Result with electrical imaging (FMI) tool

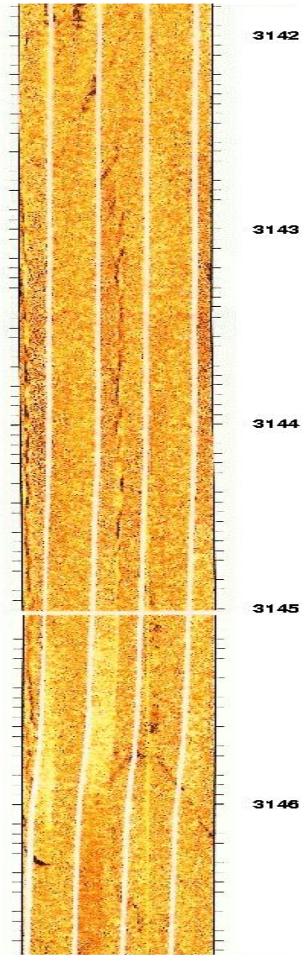


- drilling Induced fractures : thermal cooling caused by drilling

  $-\sigma_H + 3\,\sigma_h - P_b - f(P_0) - \alpha E \Delta\theta \,/\, (1-\nu) = \sigma^T$
  Where $\Delta\theta$ is the cooling of the rock

- From a Bore HoleTeleViewer (BHTV) log run in GPK1 down to 2000 m, Mastin and Heineman (1988) determine a mean direction for drilling induced fractures = N 169° ± 7°

- From FMI log run from 1500 m down to 3500 m, Brudy and Zoback find that the mean orientation of drilling induced fractures is N 181 ± 22 °

# Compression breakouts observed in well GPK1 around 3440 m

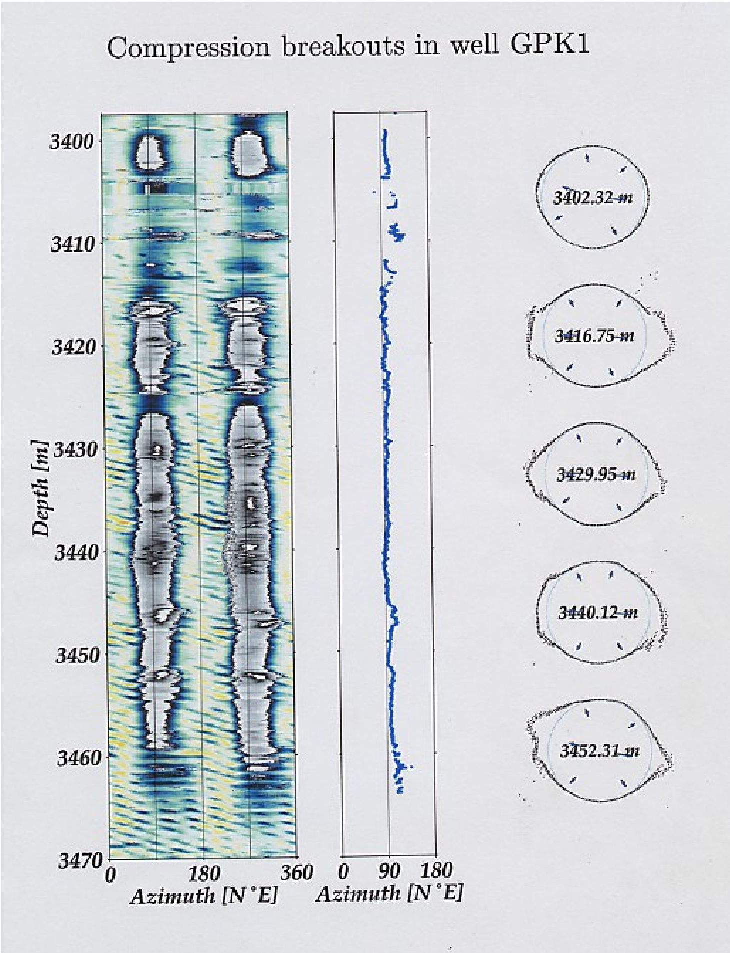


- Compression breakouts are indicative of zones of highest tangential compressive stress :

  $-\sigma_h + 3\,\sigma_H - P_b - f(P_0) - \alpha E \Delta\theta / (1-\nu) = \sigma^c$

- No breakouts seen initially in GPK1, No breakouts in GPK2 just after drilling, some seen sometime after drilling : problem of time dependency for breakout development.

- Recall loading rate effect on rock strength (e.g. Hudson & Brown, 1973)

# Borehole elongation observed in well GK2 between 1600 m and 2900 m

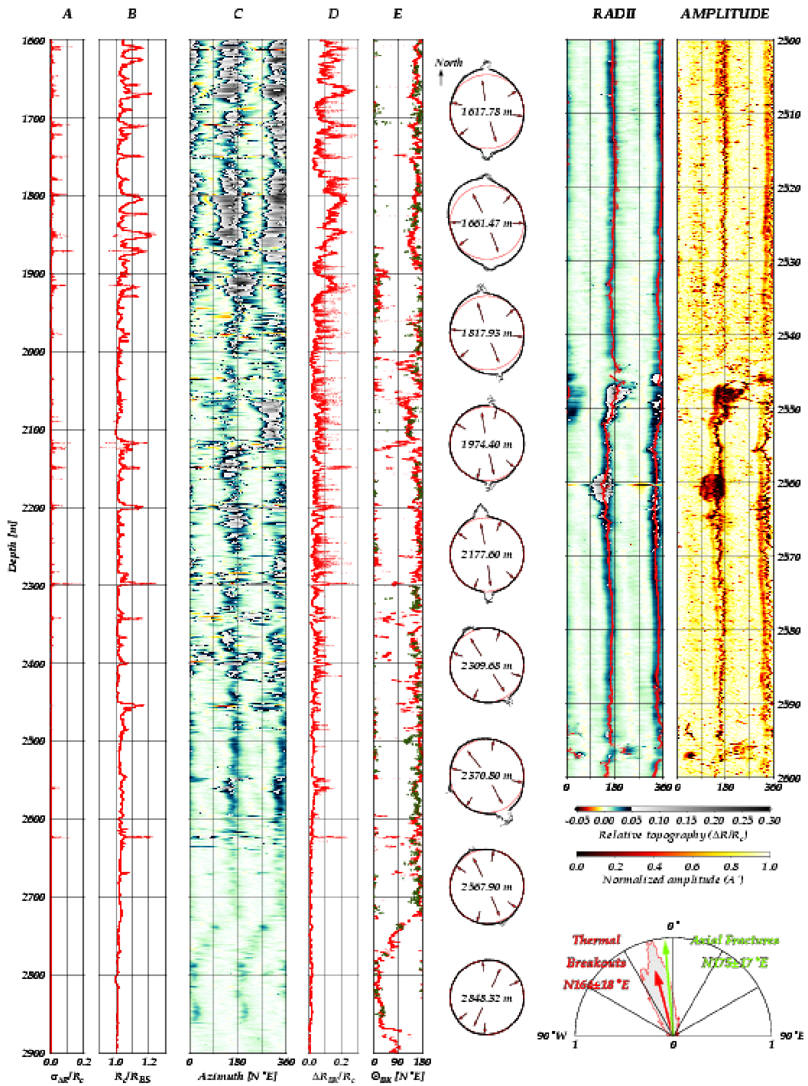

# Analysis of wellbore failure mechanisms : tensile failure and compressive failure

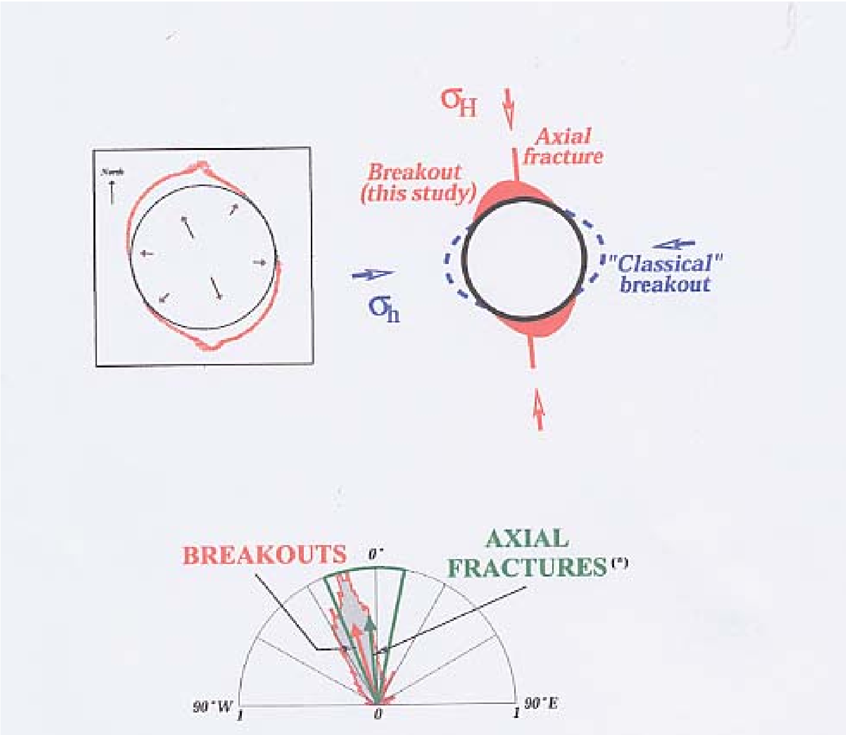


- Tangential stress at the borehole wall

  $\sigma_{\theta\theta} = (\sigma_h + \sigma_H) - 2\,(\sigma_H - \sigma_h)\cos 2\theta - P_b -$
  $f(P_0) - \alpha E \Delta\theta / (1-\nu) - 3/8\ \Delta\alpha E/(1-\nu)\ \Delta\theta$

  Where $\Delta\alpha$ is the mismatch between thermal expansion coefficients (solution for square inclusion in an homogeneous matrix)

- Time dependency of cooling :
  - Slow cooling yields borehole elongation (thermal breakouts),
  - fast cooling yields macroscopic thermal cracking

# Variation with depth of thermal perturbation in well GPK2

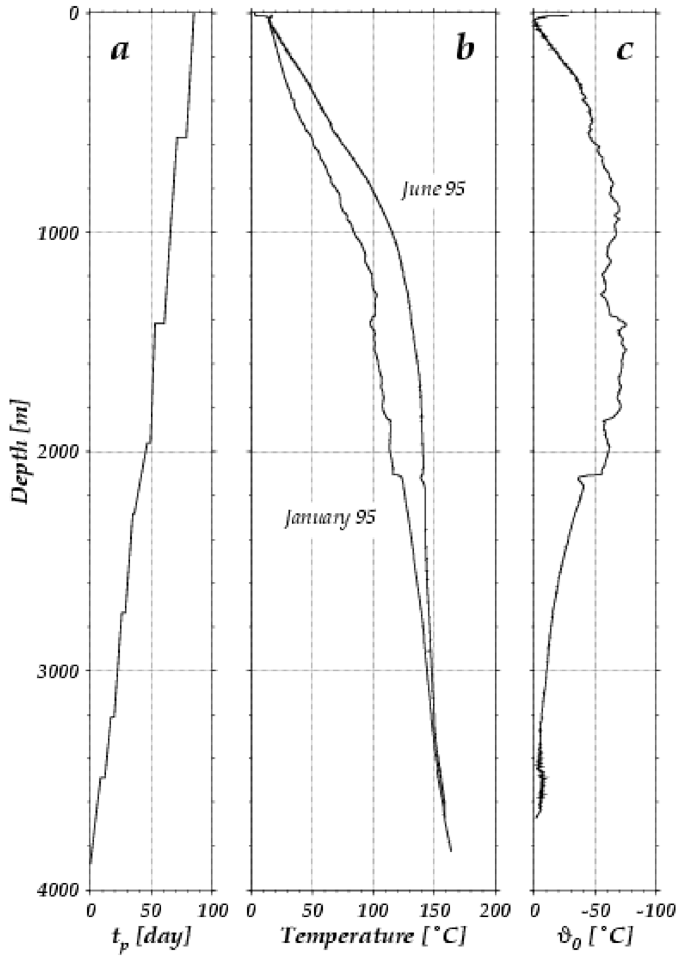


- a) Time of exposure to drilling mud circulation
- b) Thermal recovery after drilling :
  - January 95 is 3 days after the end of drilling
  - June 95 may be considered close to equilibrium (129 days after well completion)
- **C)** Variation of temperature perturbation with depth.  Can it be used for stress magnitude determination ?
- On the problem of time dependency and stress corrosion on “strength” :
  - In tension
  - In compression

# Results from large scale hydraulic reconnaissance test (2850-3400 m) (Sept. 1993)

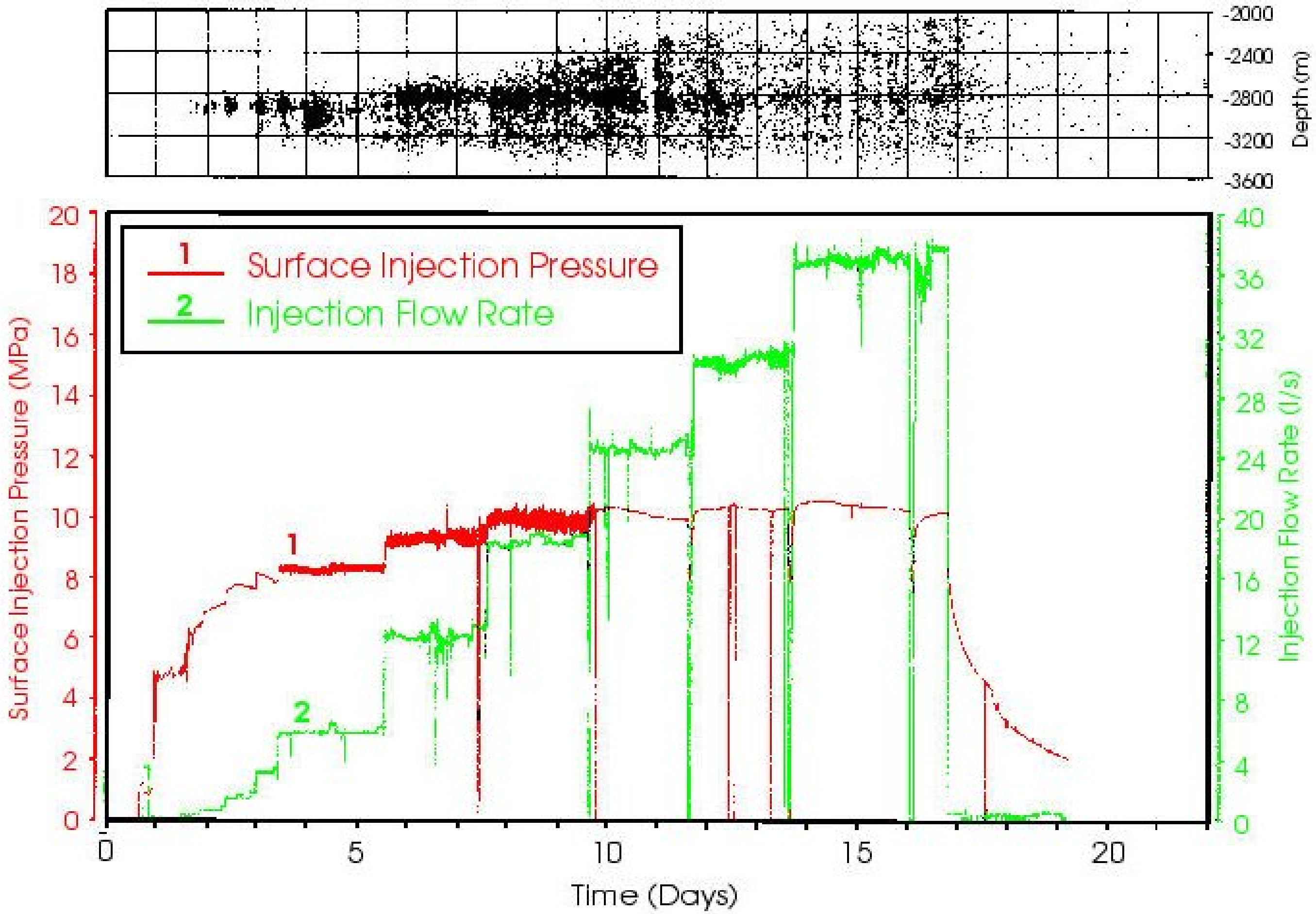

# Location of induced microseismic events

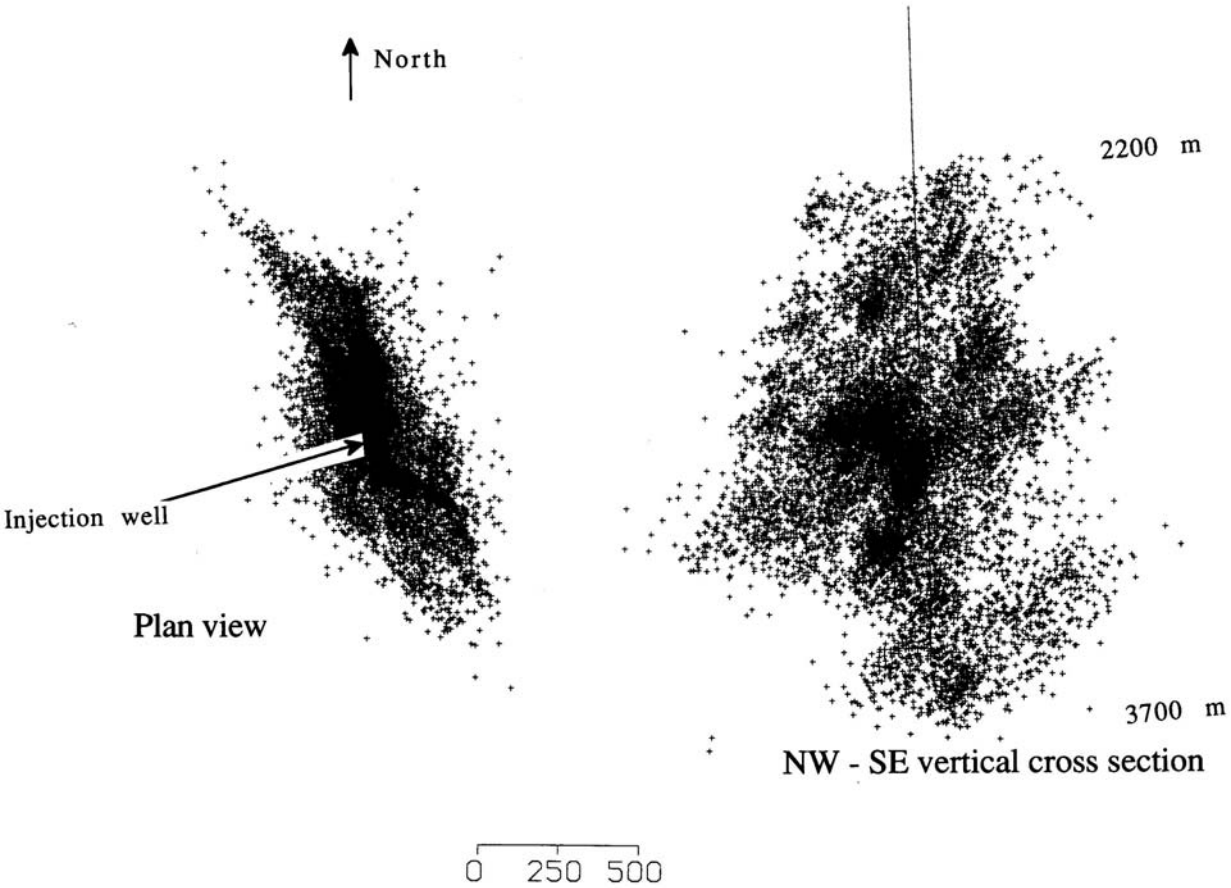


Location of induced seismicity

# Closer analysis of horizontal direction of microseismic cloud

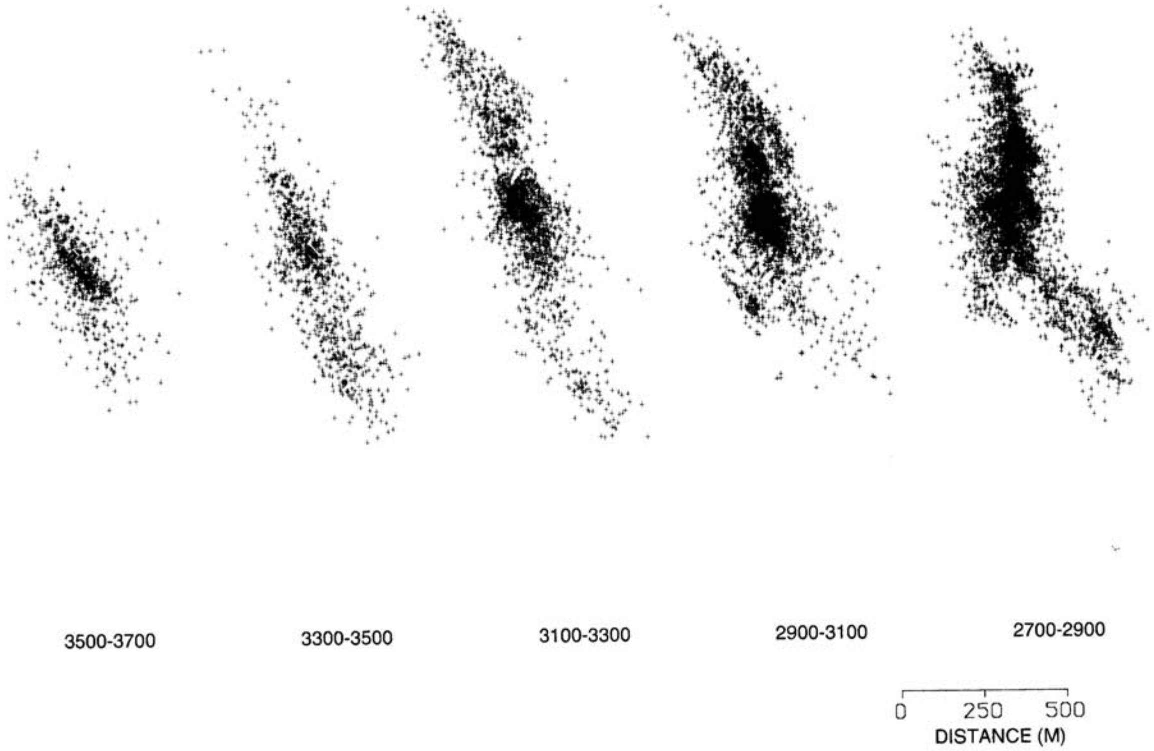

# Flow rate measurements during the test

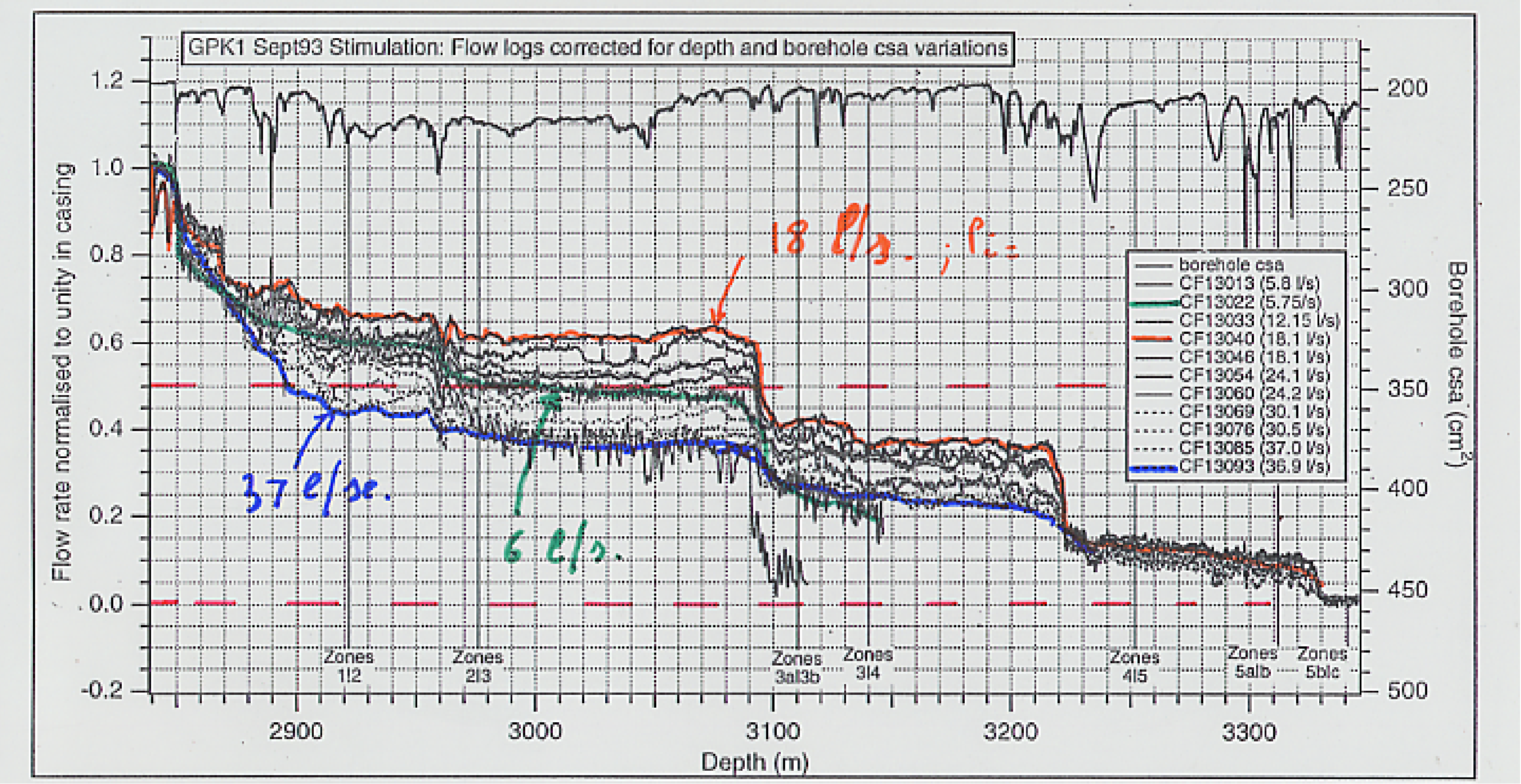

# Evaluating the regional stress field

- Mean stress direction and local heterogeneity :
  - On the role of faults on stress reorientation
  - How valid is the rock mass continuity hypothesis
  - Consequences for focal plane inversions

- Stress magnitudes evaluation
  - Vertical stress component
  - Minimum principal stress magnitude
  - Maximum principal stress magnitude

# Heterogenity in stress direction

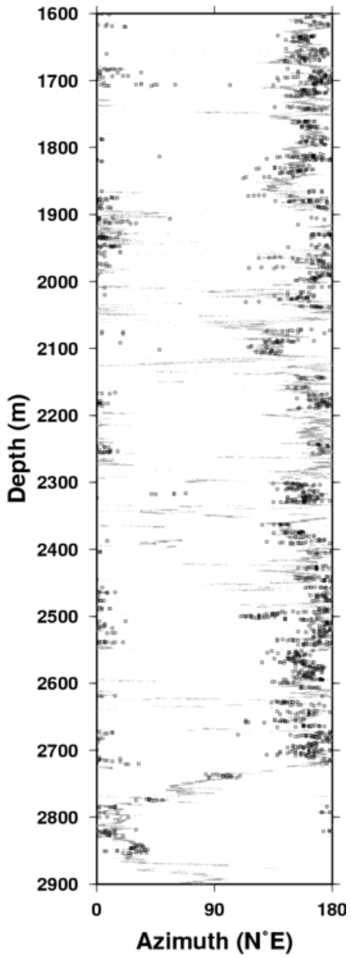


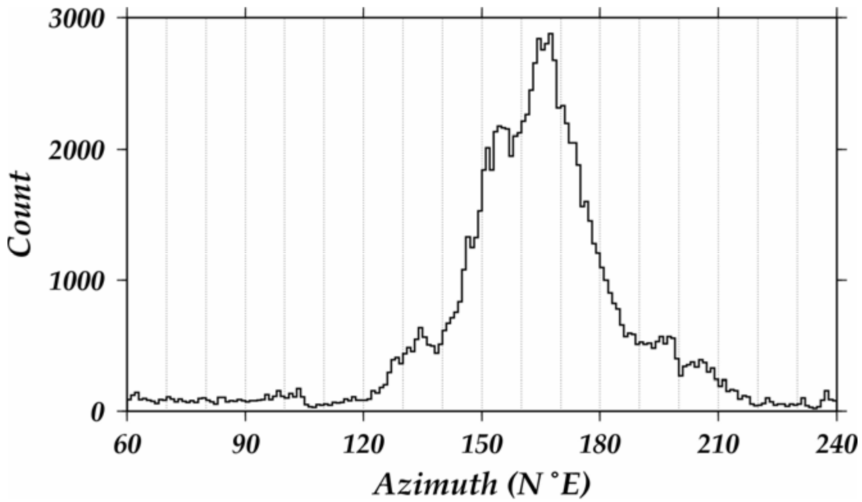

# Analysis of fault plane solutions from induced microseismicity

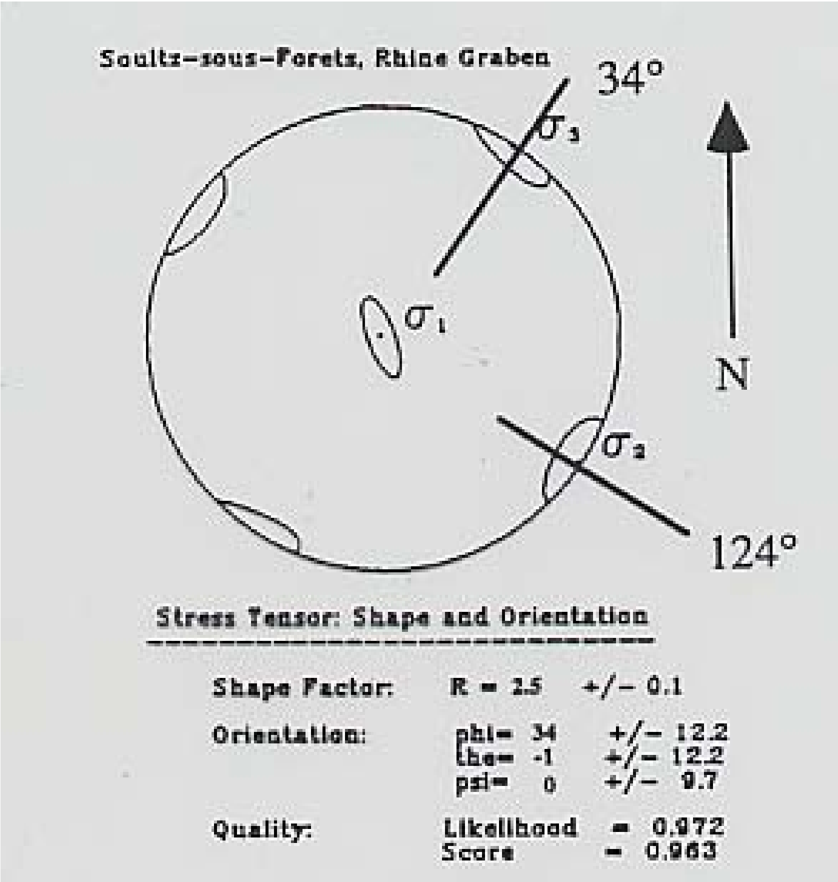


- 2 nodal planes for each focal mechanism
- Slip vector **S** in nodal plane is parallel to resolved shear stress $\tau$ in nodal plane

  **S . $\tau$ / | $\tau$ | = 1**

  **$\tau$ = Tn – (Tn.n)n**

$$(\sigma) = \sigma_1(1) + (\sigma_3 - \sigma_1)\begin{pmatrix} 0 & & \\ & 1 & \\ & & R \end{pmatrix};$$

$$R = (\sigma_2 - \sigma_1)/(\sigma_3 - \sigma_1)$$

# Focal mechanisms and stress directions

- Stress perturbation caused by previous events

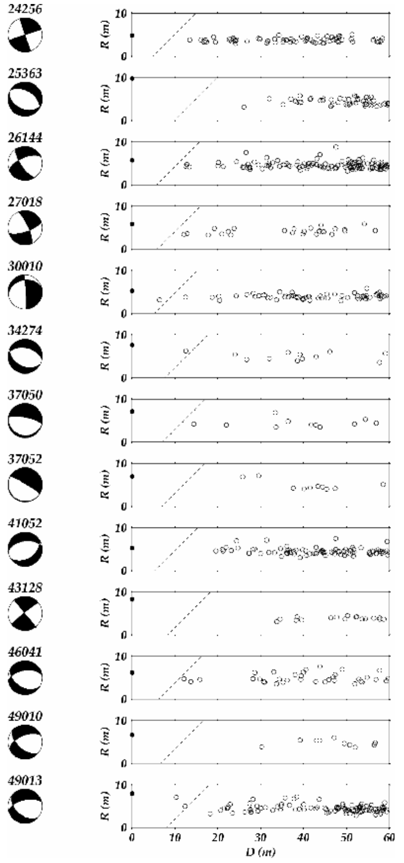


- Characterization of preexisting stress heterogeneity

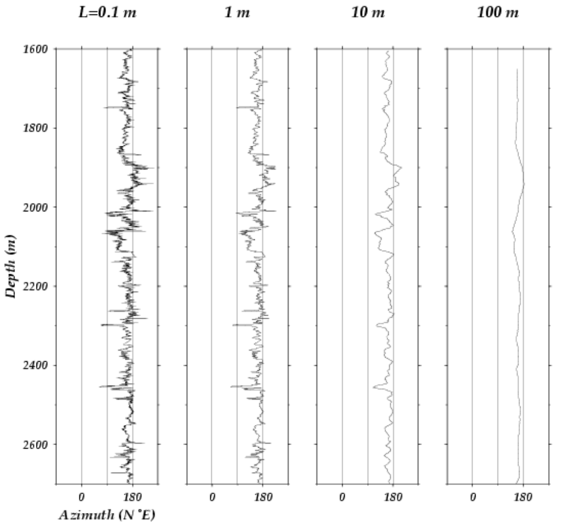


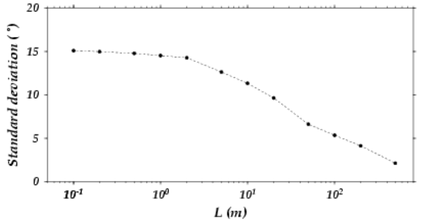

# Principal stress direction determination from shear wave splitting analysis

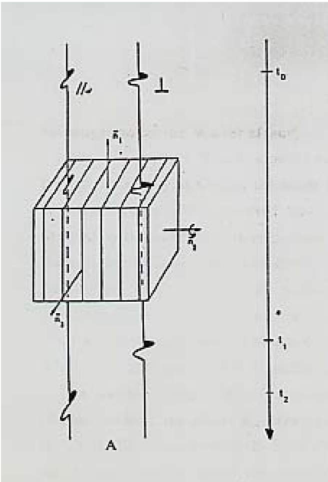

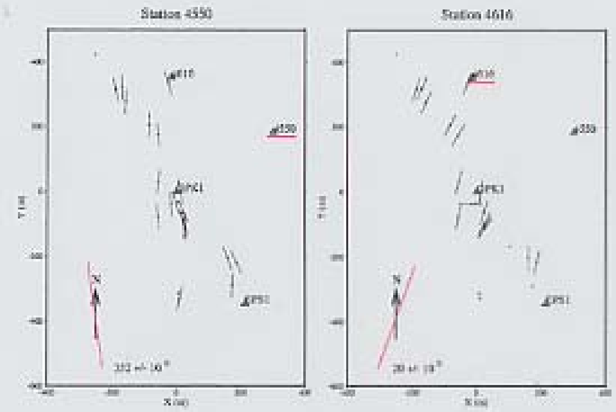


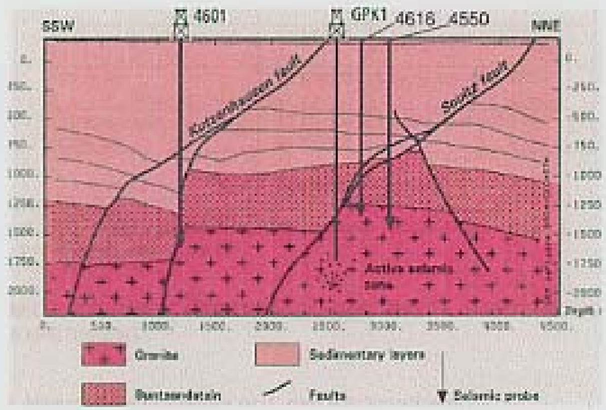


- S wave splitting

⇐ hexagonal anisotropy with a N-S horizontal symmetry axis, consistent with $\sigma_H$

- Stress rotation

⇐ topography of the sediment-granite boundary

# Comparison with other regional stress determination

- Results from Urach, from borehole breakouts between 1900 m and 3500 m (Heinemann et al., 1992) : N 172 ± 17°N

- Results from KTB (Brudy et al., 1999)

  Hydraulic fractures down to 3000 m : N 149°± 15

  Drilling induced fractures from 3000 m to 4000 m : N 154°± 17

  drilling induced fractures from 3000 to 6000 m : N 166° ± 17°

  Drilling induced fractures at 7000 m : N 182°± 21

  Drilling induced fractures at 7 800 m : N 177°± 11°

  Borehole breakouts in the upper part of well : N 149° ±18°

  Borehole breakouts around 8000 m : N 171° ± 17

# Stress magnitudes

- Why not HTPF ?

$S_v = 33.8 + 0.0255\ (z\text{-}1377);$

z in m; all stress components in MPa

- At 1980 m, $S_h/S_v = 0.535$
- At 2850 m, $S_h/S_v = 0.548$
- At 3315 m, $S_h/S_v = 0.541$

Proposition :

$S_h = 0.54\ (33.8 + 0.0255\ (z\text{-}1377))$

- In summer 2003 , at 4550 m : $S_h/S_v = 0.537$

$S_H$ magnitude from focal mechanisms and shear wave splitting:

$0.95\ S_v \leq S_H \leq 1.15\ S_v$

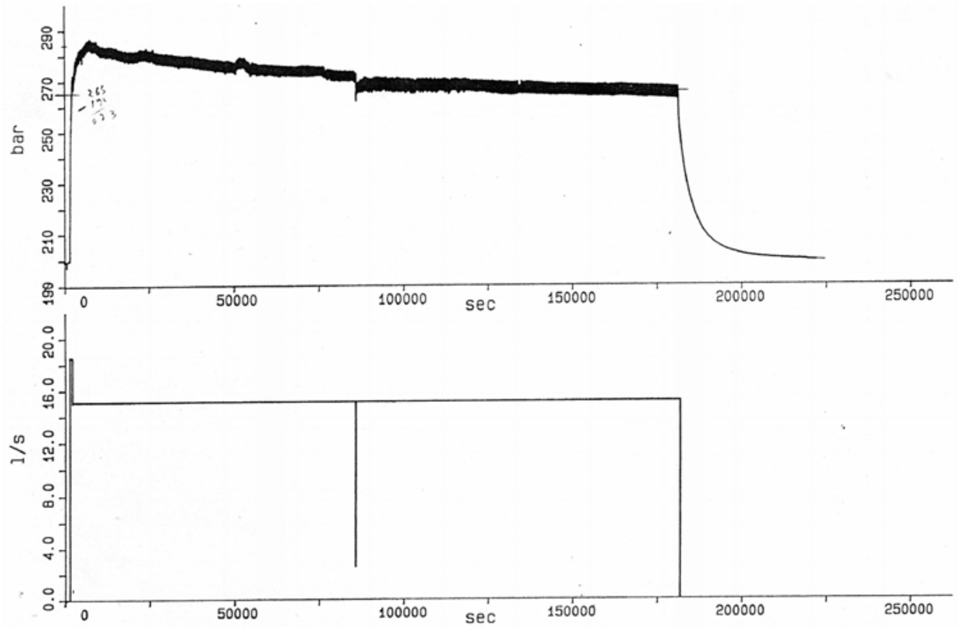


From Jung (1990) :

refrac test at 1980 m, Sh=26.5 MPa

# What failure criterion for the Granite

- Induced seismicity and rock failure
- Fault geometry and event relocation
- What failure criterion ?
- What controls stress variations with deph ?

# Acoustic emission during triaxial testing

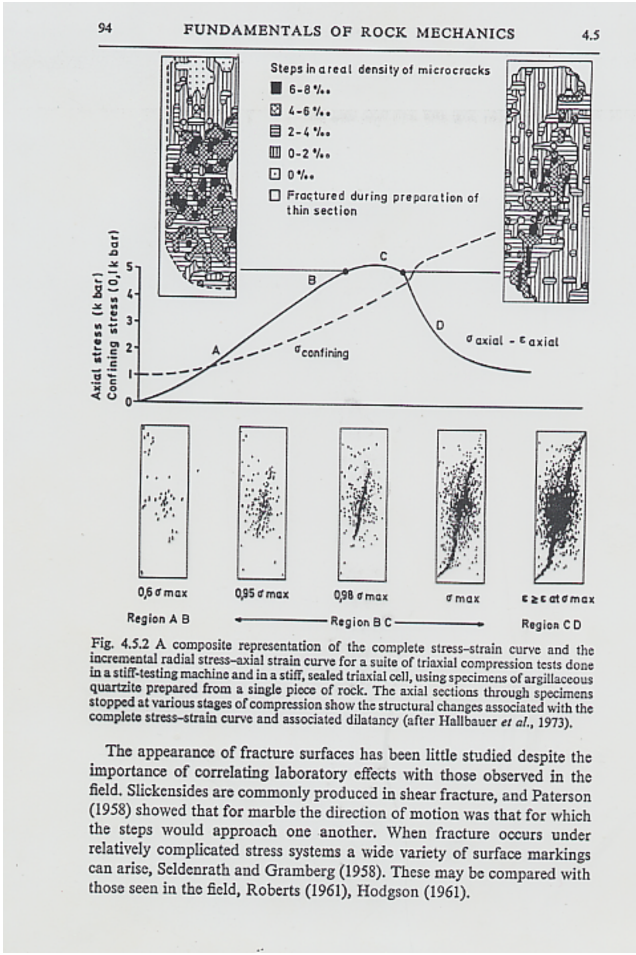





Fig. 4.5.2 A composite representation of the complete stress–strain curve and the incremental radial stress–axial strain curve for a suite of triaxial compression tests done in a stiff-testing machine and in a stiff, sealed triaxial cell, using specimens of argillaceous quartzite prepared from a single piece of rock. The axial sections through specimens stopped at various stages of compression show the structural changes associated with the complete stress–strain curve and associated dilatancy (after Hallbauer *et al.*, 1973).

The appearance of fracture surfaces has been little studied despite the importance of correlating laboratory effects with those observed in the field. Slickensides are commonly produced in shear fracture, and Paterson (1958) showed that for marble the direction of motion was that for which the steps would approach one another. When fracture occurs under relatively complicated stress systems a wide variety of surface markings can arise, Seldenrath and Gramberg (1958). These may be compared with those seen in the field, Roberts (1961), Hodgson (1961).

# Fluid flow and induced seismicity

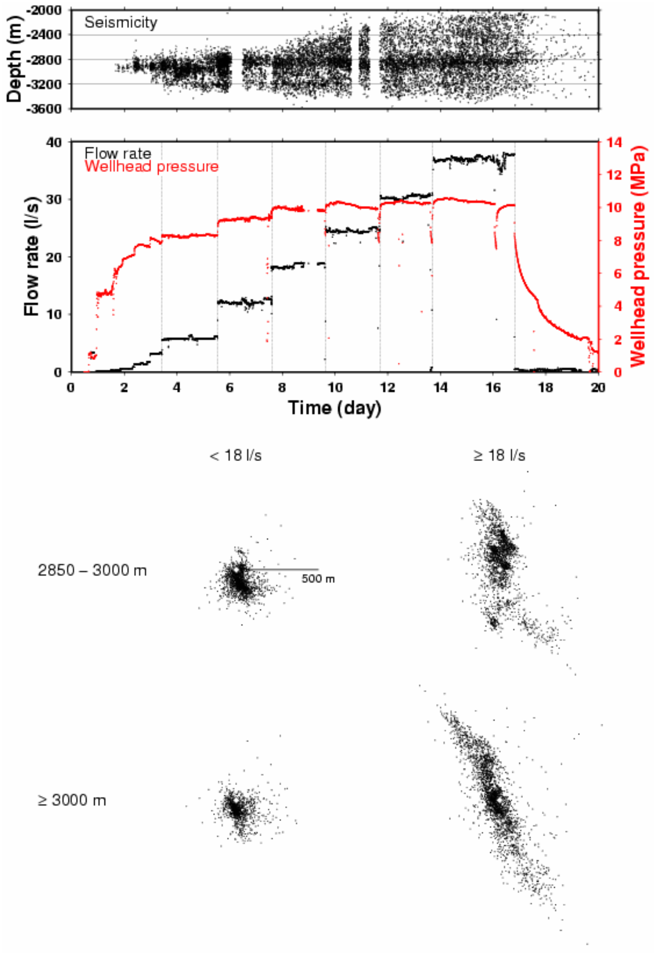

# Multiplets and events relocation

- Doublets = 2 seismic events that occur on the same asperity
- Multiplets, a series of seismic events with nearly the same source
- Cross correlation provides accurate time picking procedure for accurate relative relocation
- From relative relocation identify best fracture plane, but also relocate events with respect to main event of cluster. Then optimize relocation of main events of all clusters

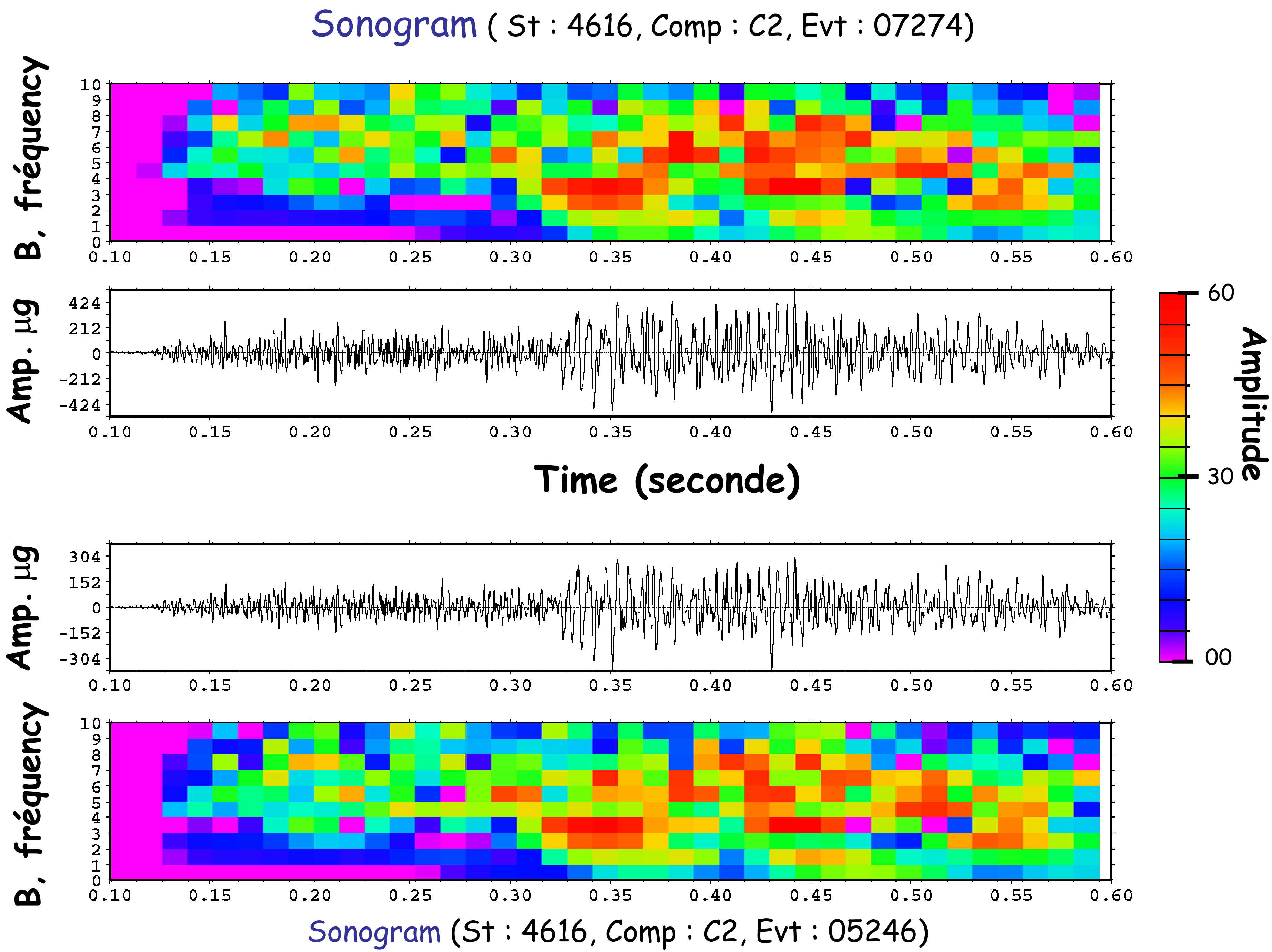

Sonogram ( St : 4616, Comp : C2, Evt : 07274)
B, fréquency
Amp. µg
424
212
0
-212
-424
0.10 0.15 0.20 0.25 0.30 0.35 0.40 0.45 0.50 0.55 0.60
Time (seconde)
Amplitude
60
30
00
304
152
-152
-304
Sonogram (St : 4616, Comp : C2, Evt : 05246)

# Multiplets

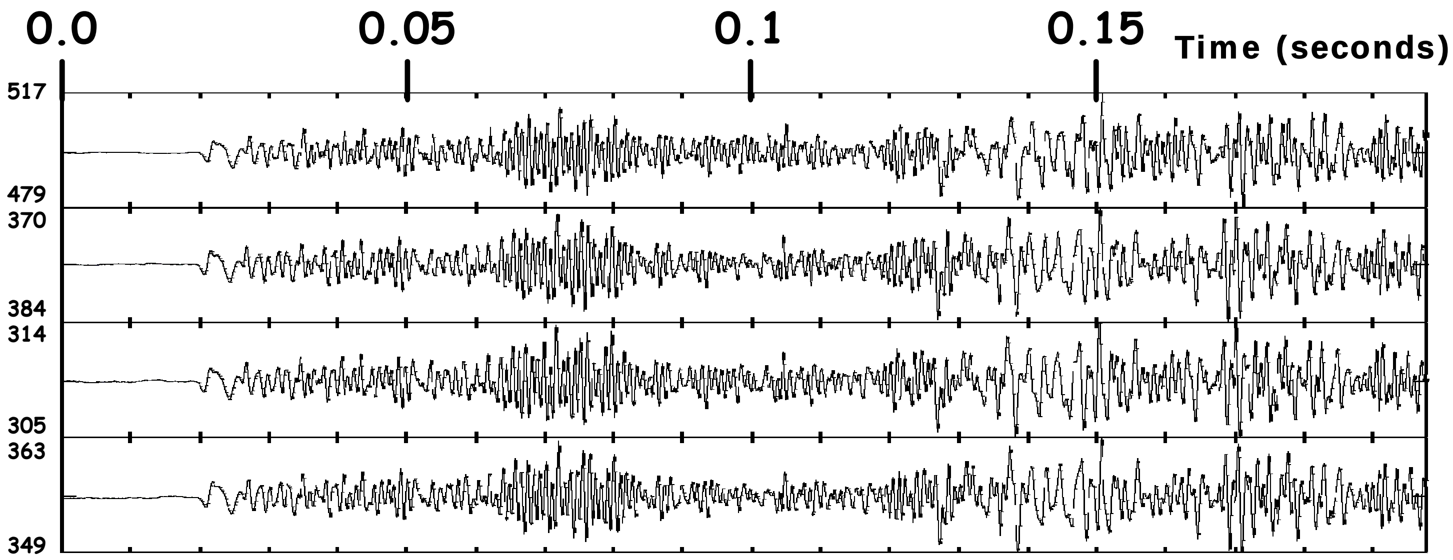

Station 4550, Z component, amplitude in ($\mu$g)

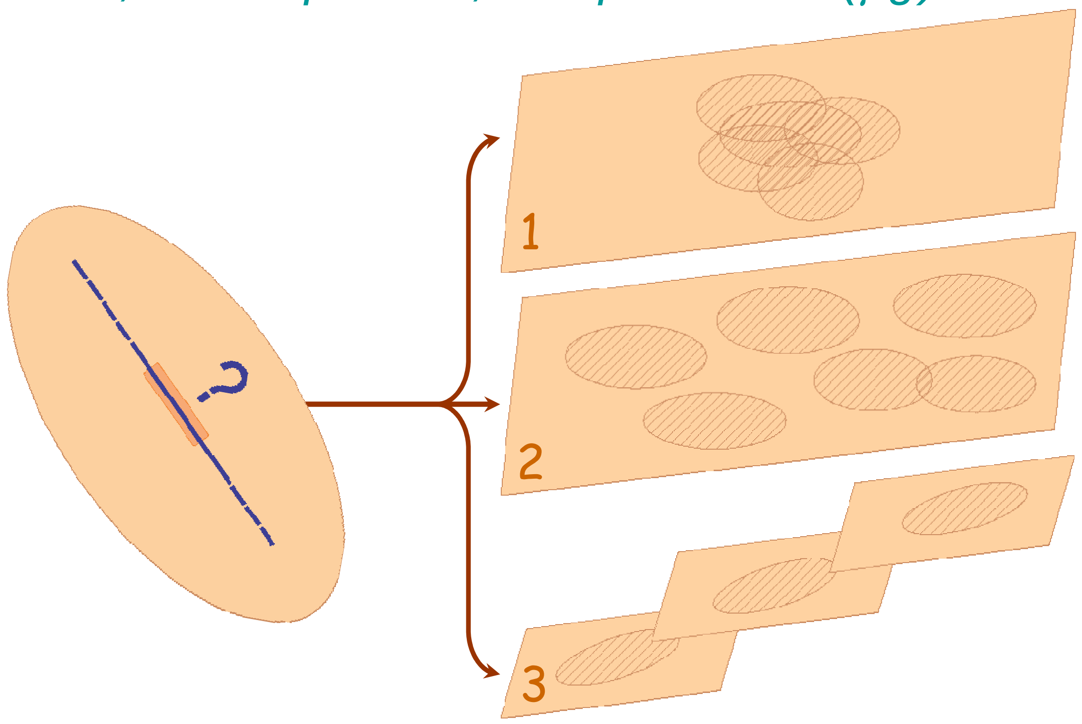


spatially close,

same source mechanism,

similar time series.

# Results from the search for multiplets

❑ Levenstein distance: 4e04

- 597 : Doublets,
- 236 : Triplets
- 128 : Quadruplets
- 222 : Multiplets (≥ 5)

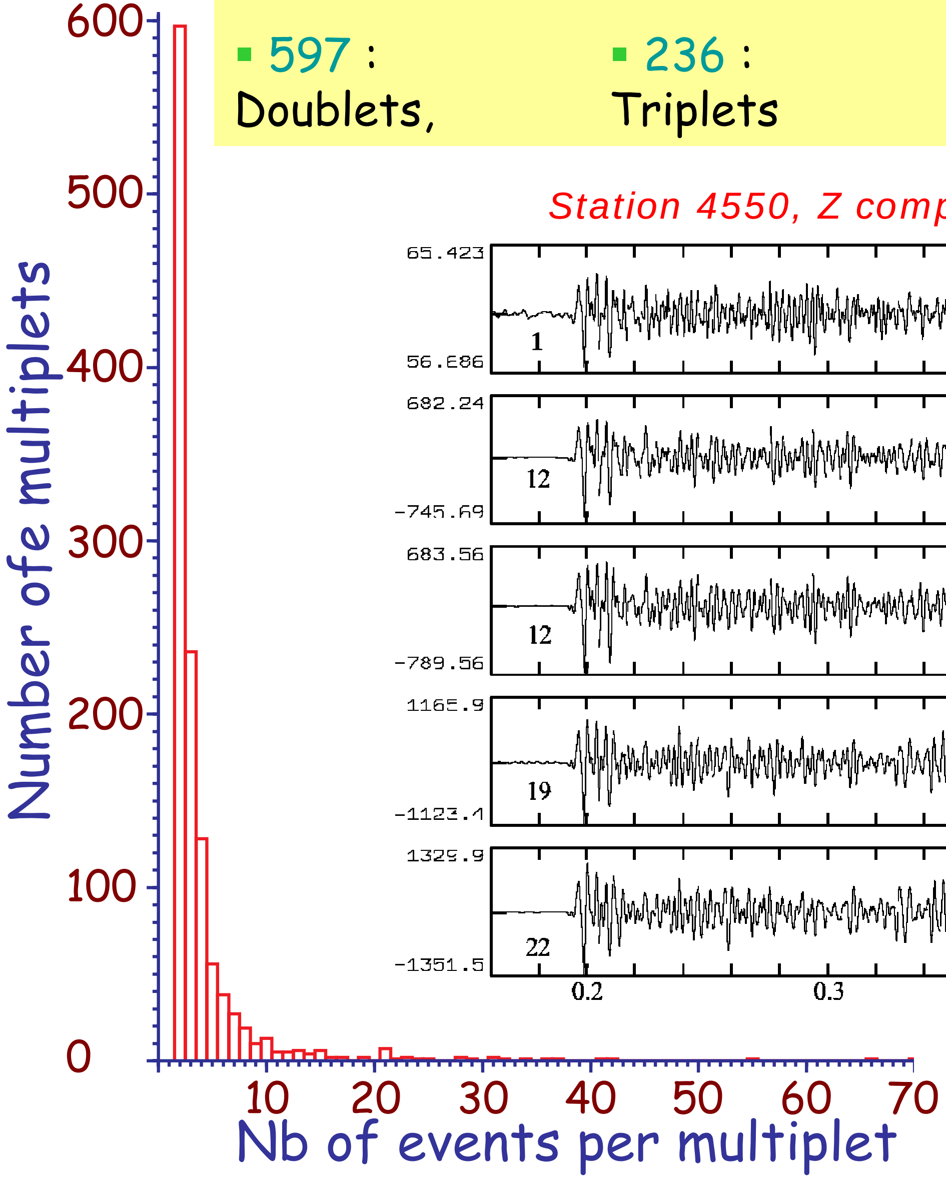


*Station 4550, Z component, amplitude in $\mu g$, Time in seconds*

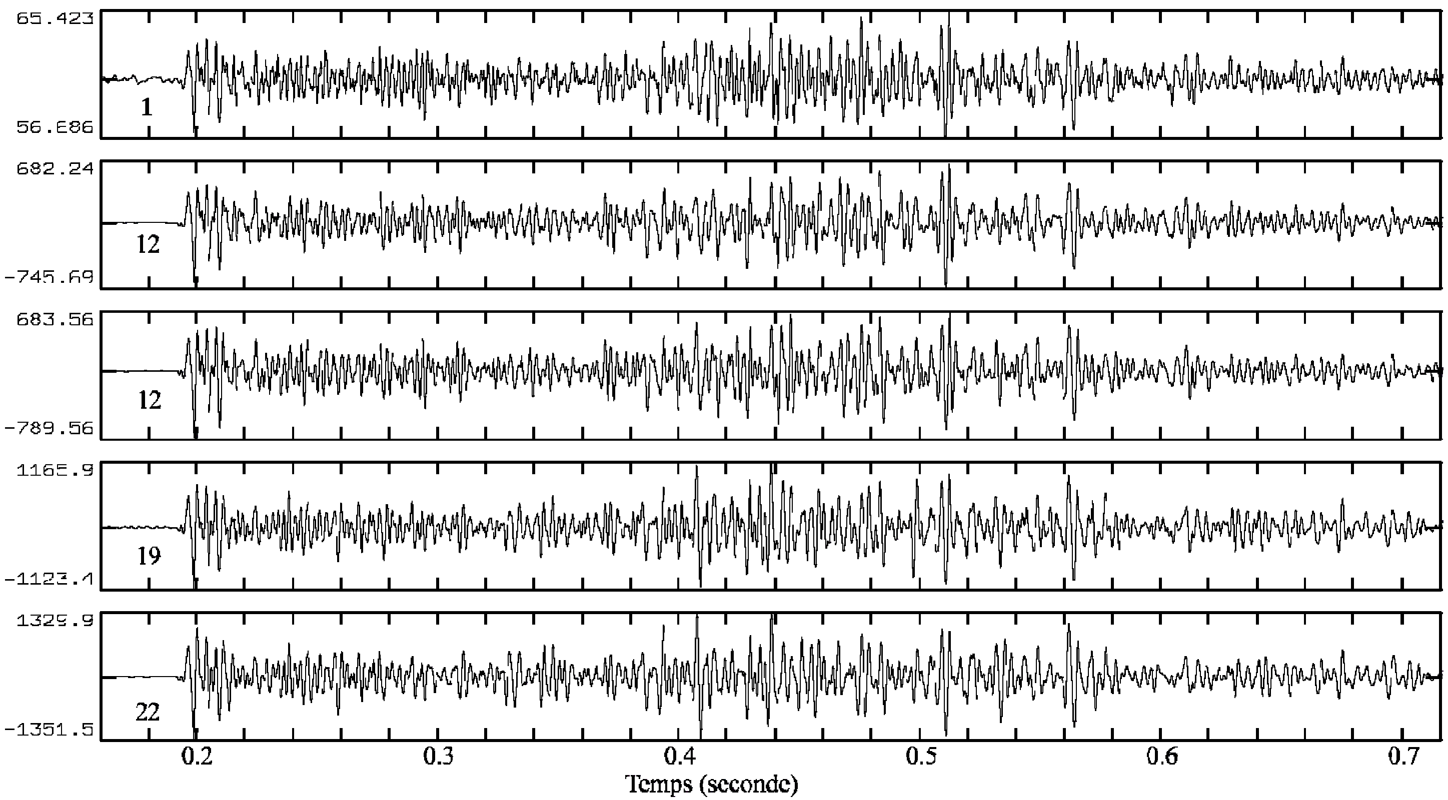

# Accurate relocation by cross correlation

- Hypothesis : no variation with time of velocity field.
- Events are close, so that rays are parallel, at receptor.
- Accuracy of relative travel times :
  - Time correlation :
    - 1 sample = ± 0.2 ms
  - Spectral cross correlation:
    - 1/20 sample = ± 0.01 ms

- Relative relocation :

$\Delta t_i = \Delta t_0 - N_x/V_i\ X_S - N_y/V_i\ Y_S - N_z/V_i\ Z_S$

$\Delta t_i$ = Difference in arrival times between Master and Slave, I = P or S;

$\Delta t_0$ difference of time occurrence between Master and Slave.

subtracting $\Delta t_p$ from $\Delta t_s$ eliminates $\Delta t_0$ and provides means to determine $X_s$, $Y_s$, $Z_s$

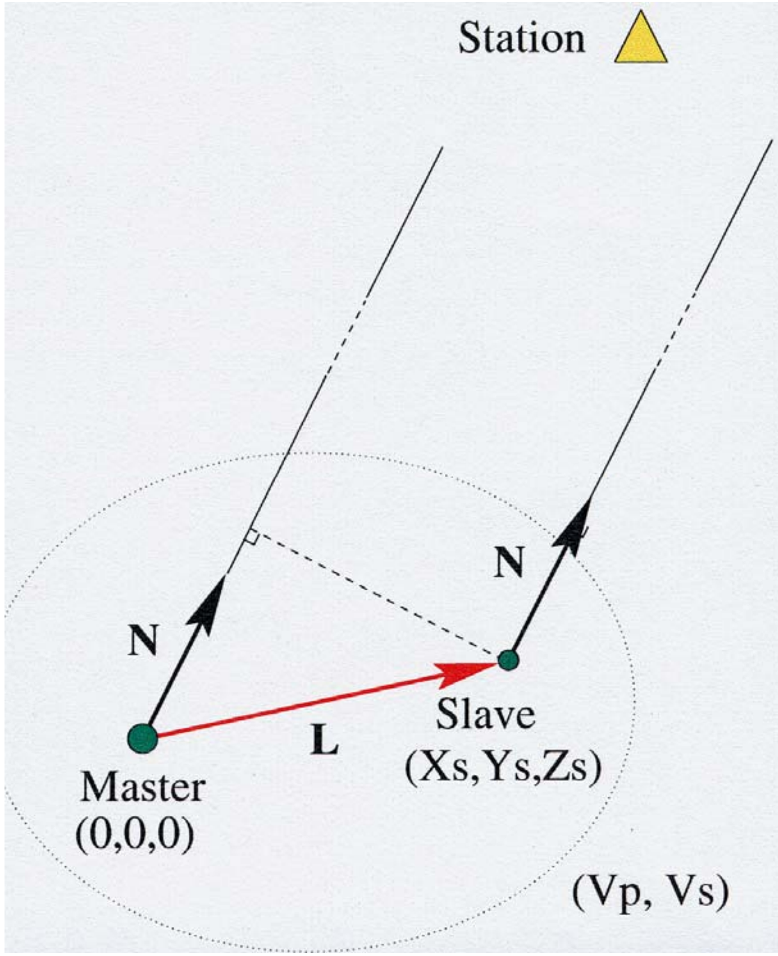

# Identification of fracture zones

## 1. For each multiplet

One multiplet characterizes one single plane (or one line)

linear regression (Tarantola 1987; Gaucher, 1998).

$$\alpha x + \beta y + \gamma z = 1$$

↳ best plane.

- Three points method (Fehler et al, 1975)

$$n(n-1)(n-2)/6$$

↳ identifies the direction that has been picked the most often.

## 2. Combine multiplets for a given depth interval and use 3 points methods for all events

# Identifying the fault plane geometry

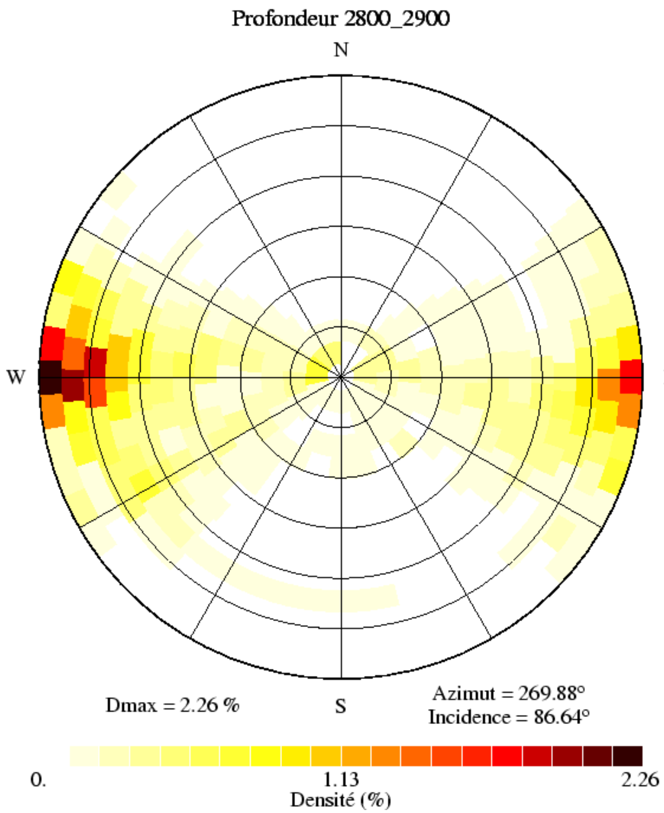


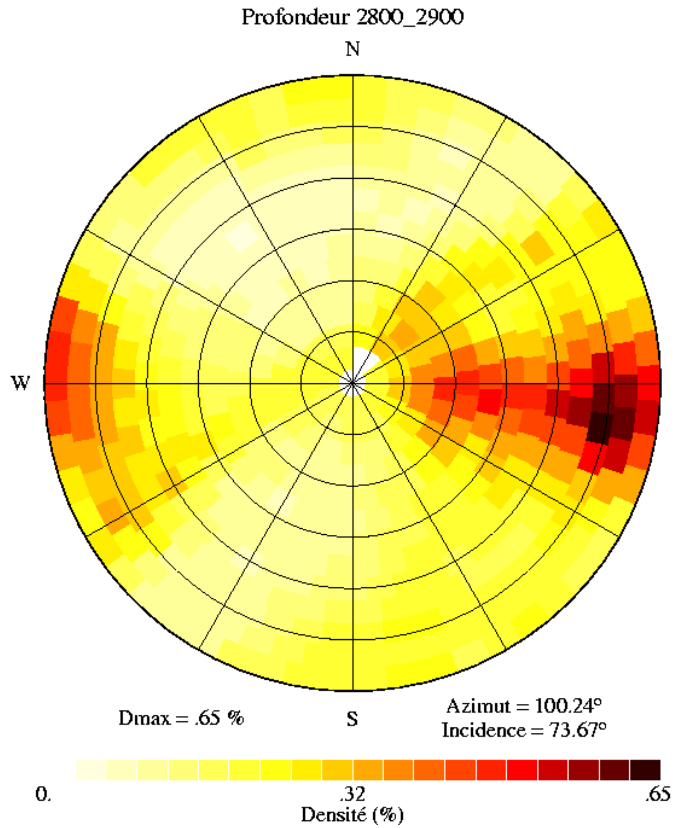

# Change of orientation with depth

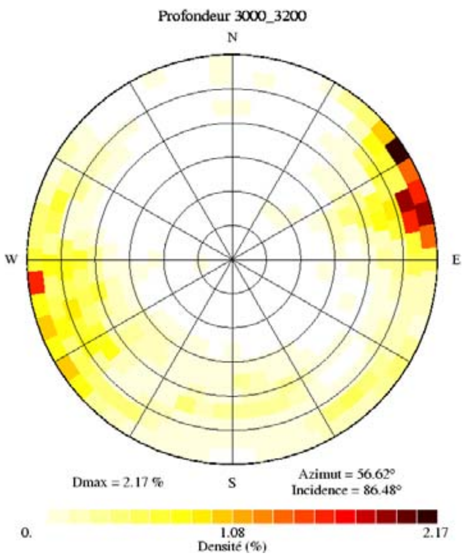


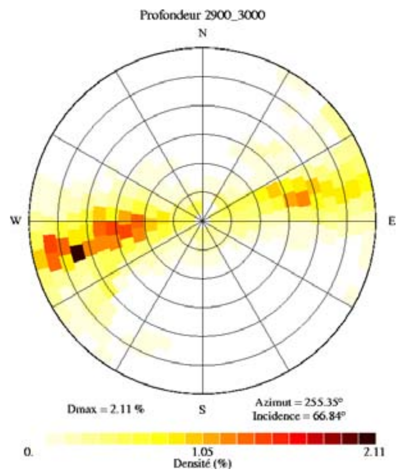


| Depth interval (m)l | Mean azimuth | Mean dip | Number of events |
|---|---|---|---|
| 2800 - 2900 | N179°E | 87° | 329 |
| 2900 – 3000 | N165°E | 67° | 402 |
| 3000 - 3200 | N146°E | 86° | 416 |
| | | | |
| 1990 - 2200 | N 147°E | 87° | |

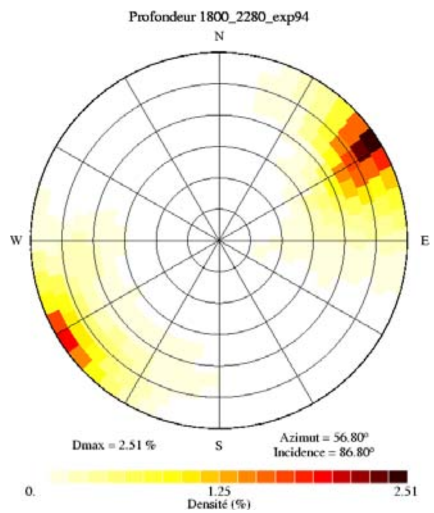

# What failure criterion ?

Byerlee's law or Mohr-Coulomb ?

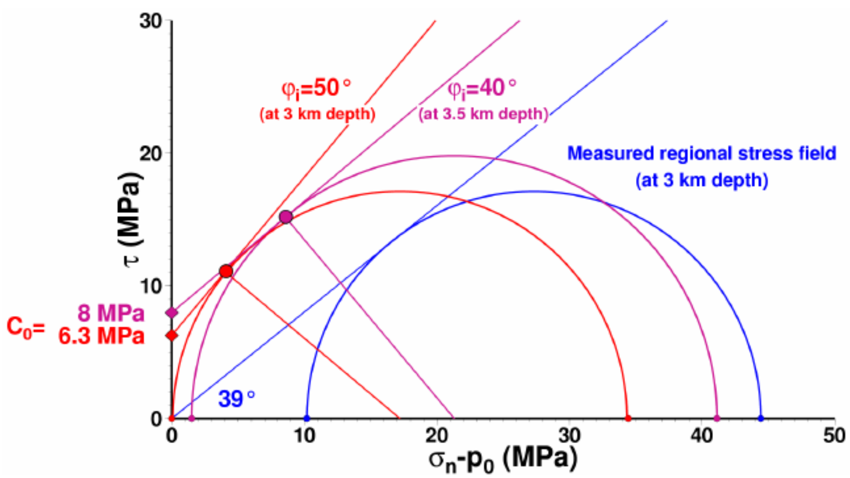


Evaluation of the rock mass permeability from the rate of growth of the microseismic cloud (Shapiro et al., 2000) yields pore pressure at time of failure inception

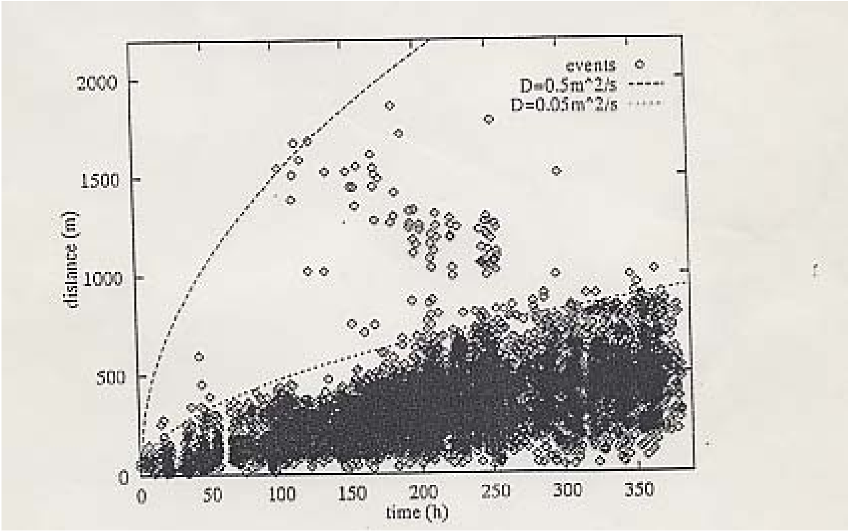

# Conclusions from Soultz

- On principal stress directions at depth (below 2000 m) :

  in western central Europe : N 170 ± 10 E

- On inversion of focal plane solutions : beware local stress heterogeneity (source size > 50 m).

- On vertical stress profile : linearity comes from visco-elasticity rather than friction, since rock mass is not at failure.